Modeling Asymmetric Tail Risk in Equity Markets with a Copula–GARCH Framework

AUTHOR
Laura Anedda

ABSTRACT
This report investigates the joint dynamics of the S&P 500 (^GSPC) and STOXX Europe 600 (^STOXX) equity indices from 1 January 2010 to the present. A two-stage Copula–GARCH framework is employed: first, marginal conditional heteroskedasticity is modeled using univariate GARCH(1,1) processes; second, the standardized innovations are coupled via a variety of parametric copulas (Gaussian, Student-t, and Archimedean families). Model selection is guided by information criteria and tail-dependence diagnostics. A Monte Carlo simulation is performed to assess joint tail risk, highlighting how standard VaR metrics may underestimate portfolio risk under the false assumption of independence. The analysis quantifies the probability of simultaneous 95% drawdowns across both indices and reveals a significant tail-dependence penalty. Building on this, the study develops a conditional probability-based trading strategy that exploits short-term pricing dislocations between the two assets. By interpreting asymmetric tail events as signals of relative mispricing, the framework generates systematic long/short positions aimed at capturing mean-reverting behaviour implied by the joint distribution. This end-to-end approach provides insights for both risk management and tactical allocation under extreme co-movement regimes.

0. Introduction

Assessing joint tail risk—the probability of extreme losses occurring simultaneously across multiple assets—is a critical challenge in financial risk management. Standard Value at Risk (VaR) methods often assume independence among asset returns, leading to a potential underestimation of portfolio risk, especially under stress conditions when dependencies tend to strengthen. Empirical evidence shows that during market turmoil, asset returns frequently exhibit nonlinear dependencies and joint extreme behavior that cannot be captured by models relying on simple correlation or Gaussian assumptions.

To address these limitations, this study employs a Copula-GARCH framework, which separates the modeling of marginal volatility dynamics from the cross-sectional dependence structure. Univariate GARCH models are employed to capture the heteroskedastic and clustered volatility patterns typical of financial time series. The residuals from these models are transformed using the Probability Integral Transform (PIT) and used to estimate a copula, which allows for the modeling of complex, non-linear, and asymmetric dependence structures, including tail dependence.

The methodological workflow implemented in this study proceeds as follows:

- **Data Preparation**: Log-returns of two equity indices are computed and preprocessed.
- **Marginal Modeling**: Each return series is modeled using a GARCH(1,1) process to account for conditional volatility dynamics.
- **Model Selection:** Diagnostics are conducted to assess the adequacy of the marginal models and select the best specifications.
- **Copula Estimation:** Standardized residuals are transformed via PIT, and several copula families (Gaussian, Student-t, Archimedean) are fitted. Selection is guided by information criteria (e.g., AIC) and tail dependence diagnostics.
- **Monte Carlo Simulation:** 10,000 joint scenarios are simulated using the selected copula and inverted back to the original return scale using the GARCH marginals.
- **Joint Tail Risk Estimation:** The empirical probability of both assets breaching their respective 95% VaR thresholds is computed and compared to the theoretical benchmark under independence (0.0025), illustrating the importance of correctly modeling dependence.

- **Trading Signal Generation:** Based on the copula-implied conditional probabilities, relative-value trading signals are constructed. Positions are taken only when strong asymmetries in joint tail behaviour are detected, exploiting short-term dislocations between the two assets through systematic long/short allocations.

---

1. Data Preparation

Let $P_t^{(i)}$ denote the adjusted closing price of asset i on trading day t. We retrieve adjusted closing prices, ensuring dividend and split adjustments. This yields two price series, $P_t^{(1)} = P_{SP,t}$ and $P_t^{(2)} = P_{STOXX,t}$, for subsequent return calculation.

Under the **efficient-markets hypothesis** prices follow a forward-looking martingale difference sequence, but not necessarily with homoskedastic increments, motivating the volatility model introduced next.

Returns Calculation

For each series we construct continuously compounded (log) returns

$$r_t^{(i)} = \ln P_t^{(i)} - \ln P_{t-1}^{(i)}, \qquad i \in \{1, 2\}.$$

Logarithmic scaling ensures (i) additivity over time, (ii) approximation to simple returns for small price moves, (iii) symmetry of positive and negative innovations in the neighborhood of zero.

The return vector is

$$\boldsymbol{r}_t = \begin{pmatrix} r_t^{(1)} \\ r_t^{(2)} \end{pmatrix}, \qquad t = 2, \ldots, T.$$

Missing values introduced by non-synchronous holidays are removed via *listwise deletion*, yielding a balanced panel of joint observations:

$$\boldsymbol{r} = \{\boldsymbol{r}_t\}_{t=2}^{T}.$$

---

2. Marginal Models for Volatility Dynamics

The first stage of our Copula-GARCH framework involves modeling the marginal volatility dynamics of each return series. We consider three GARCH specifications combined with six different distributions for the innovations.

2.1 GARCH Model Specifications

Standard GARCH(1,1)

The basic GARCH(1,1) model assumes:

$$\begin{aligned} r_t &= \sigma_t z_t \\ \sigma_t^2 &= \omega + \alpha r_{t-1}^2 + \beta \sigma_{t-1}^2 \end{aligned}$$

where $\omega > 0$, $\alpha, \beta \geq 0$, and $\alpha + \beta < 1$ for stationarity.

GJR-GARCH(1,1)

This model extends standard GARCH by allowing asymmetric response to negative returns:

$$r_t = \sigma_t z_t$$
$$\sigma_t^2 = \omega + \alpha r_{t-1}^2 + \gamma r_{t-1}^2 \mathbf{1}_{r_{t-1}<0} + \beta \sigma_{t-1}^2$$

where γ captures the additional impact of negative returns ("leverage effect").

EGARCH(1,1)

The Exponential GARCH models log-volatility to ensure positivity:

$$r_t = \sigma_t z_t$$
$$\log(\sigma_t^2) = \omega + \alpha \left| \frac{r_{t-1}}{\sigma_{t-1}} \right| + \gamma \frac{r_{t-1}}{\sigma_{t-1}} + \beta \log(\sigma_{t-1}^2)$$

where γ captures asymmetric effects without requiring parameter constraints.

2.2 Innovation Distributions

For each GARCH specification, we consider six different distributions for the innovations z_t. All distributions are automatically standardized by the `rugarch` package to ensure proper scaling of the volatility process, making the conditional variance σ_t^2 interpretable across different specifications.

> **Technical note**: Standardization involves rescaling each innovation distribution so that its first two moments satisfy $\mathbb{E}[z_t] = 0$ and $\mathrm{Var}(z_t) = 1$. This allows the conditional variance σ_t^2 to reflect only the time-varying volatility, without being influenced by changes in the innovation scale or shape. This assumption follows the standard GARCH framework, where the innovations are assumed to be i.i.d. with zero mean and unit variance.

Distribution	Density.Notation	Symmetry	Tail.Behavior	Skewness	Key.Parameters	Notes
Normal	$z_t \sim \mathcal{N}(0, 1)$	Yes	Thin	No	–	Naturally standardized; often inadequate for capturing extreme market movements.
Student-t	$z_t \sim t(\nu)$	Yes	Heavy	No	ν (df)	Tail thickness controlled by degrees of freedom; better suited for extreme returns.
GED	$z_t \sim \mathrm{GED}(\nu)$	Yes	Flexible	No	ν (shape)	Includes Normal ($\nu = 2$) and Laplace ($\nu = 1$) as special cases.
Skew-Normal	$z_t \sim \mathrm{SN}(\xi)$	No	Thin	Yes	ξ (skewness)	Allows for asymmetry with relatively light tails.
Skew-Student-t	$z_t \sim \mathrm{ST}(\nu, \xi)$	No	Heavy	Yes	ν (thickness), ξ (skewness)	Combines heavy tails with asymmetry; most flexible among t-distributions.
Normal Inverse Gaussian (NIG)	$z_t \sim \mathrm{NIG}(\alpha, \beta, \mu, \delta)$	No	Very Heavy	Yes	location (μ), scale (δ), tail heaviness (α), asymmetry (β)	Captures both skewness and excess kurtosis; highly flexible and well-suited to finance.

Table 1: Innovation Distributions Considered for GARCH Models

Model selection is based on:

1. **Information Criteria**: AIC, BIC, Shibata, and Hannan-Quinn

2. **Diagnostic Tests**: - Ljung-Box test for remaining serial correlation - ARCH-LM test for remaining heteroskedasticity

The best model for each series will be selected based on the lowest AIC value among specifications that pass the diagnostic tests.

S&P 500 – Model Comparison

Model	AIC	BIC	Shibata	Hannan–Quinn
sGARCH(1,1) – Normal	-6.6047	-6.5997	-6.6047	-6.6029
sGARCH(1,1) – Student-t	-6.6586	-6.6520	-6.6586	-6.6562
sGARCH(1,1) – GED	-6.6614	-6.6547	-6.6614	-6.6590
sGARCH(1,1) – Skew-Normal	-6.6328	-6.6262	-6.6328	-6.6305
sGARCH(1,1) – Skew-Student	-6.6752	-6.6669	-6.6752	-6.6723
sGARCH(1,1) – NIG	-6.6816	-6.6733	-6.6816	-6.6786
GJR-GARCH(1,1) – Normal	-6.6421	-6.6355	-6.6421	-6.6397
GJR-GARCH(1,1) – Student-t	-6.7003	-6.6920	-6.7003	-6.6973
GJR-GARCH(1,1) – GED	-6.6953	-6.6870	-6.6953	-6.6924
GJR-GARCH(1,1) – Skew-Normal	-6.6759	-6.6676	-6.6759	-6.6730
GJR-GARCH(1,1) – Skew-Student	-6.7206	-6.7106	-6.7206	-6.7170
GJR-GARCH(1,1) – NIG	-6.7244	-6.7145	-6.7245	-6.7209
EGARCH(1,1) – Normal	-6.6505	-6.6439	-6.6505	-6.6482
EGARCH(1,1) – Student-t	-6.7071	-6.6988	-6.7071	-6.7041
EGARCH(1,1) – GED	-6.7014	-6.6931	-6.7014	-6.6984
EGARCH(1,1) – Skew-Normal	-6.6853	-6.6770	-6.6853	-6.6823
EGARCH(1,1) – Skew-Student	-6.7283	-6.7184	-6.7283	-6.7248
EGARCH(1,1) – NIG	-6.7319	-6.7219	-6.7319	-6.7283

Table 2: S&P 500 GARCH models – Information Criteria

S&P 500 – Diagnostic Tests

Model	Ljung-Box (p-value)	ARCH-LM (p-value)
sGARCH(1,1) – Normal	0.1639	0.1978
sGARCH(1,1) – Student-t	0.1728	0.3795
sGARCH(1,1) – GED	0.1709	0.3190
sGARCH(1,1) – Skew-Normal	0.1609	0.1968
sGARCH(1,1) – Skew-Student	0.1701	0.3516
sGARCH(1,1) – NIG	0.1683	0.3239
GJR-GARCH(1,1) – Normal	0.2915	0.2518
GJR-GARCH(1,1) – Student-t	0.2993	0.4140
GJR-GARCH(1,1) – GED	0.3023	0.3408
GJR-GARCH(1,1) – Skew-Normal	0.2870	0.3265
GJR-GARCH(1,1) – Skew-Student	0.2981	0.4192
GJR-GARCH(1,1) – NIG	0.2945	0.4134
EGARCH(1,1) – Normal	0.1511	0.2348
EGARCH(1,1) – Student-t	0.1605	0.1880
EGARCH(1,1) – GED	0.1644	0.2769
EGARCH(1,1) – Skew-Normal	0.1494	0.2174

EGARCH(1,1) – Skew-Student	0.1564	0.1555
EGARCH(1,1) – NIG	0.1576	0.1835

Table 3: S&P 500 GARCH models – Residual Diagnostics

STOXX 600 – Model Comparison

Model	AIC	BIC	Shibata	Hannan–Quinn
sGARCH(1,1) – Normal	-6.5527	-6.5477	-6.5527	-6.5510
sGARCH(1,1) – Student-t	-6.6036	-6.5969	-6.6036	-6.6012
sGARCH(1,1) – GED	-6.6024	-6.5957	-6.6024	-6.6000
sGARCH(1,1) – Skew-Normal	-6.5732	-6.5666	-6.5732	-6.5708
sGARCH(1,1) – Skew-Student	-6.6189	-6.6107	-6.6189	-6.6160
sGARCH(1,1) – NIG	-6.6218	-6.6136	-6.6219	-6.6189
GJR-GARCH(1,1) – Normal	-6.6009	-6.5943	-6.6009	-6.5986
GJR-GARCH(1,1) – Student-t	-6.6495	-6.6412	-6.6495	-6.6466
GJR-GARCH(1,1) – GED	-6.6425	-6.6342	-6.6425	-6.6396
GJR-GARCH(1,1) – Skew-Normal	-6.6238	-6.6155	-6.6238	-6.6209
GJR-GARCH(1,1) – Skew-Student	-6.6658	-6.6558	-6.6658	-6.6622
GJR-GARCH(1,1) – NIG	-6.6663	-6.6564	-6.6663	-6.6628
EGARCH(1,1) – Normal	-6.6134	-6.6068	-6.6134	-6.6111
EGARCH(1,1) – Student-t	-6.6607	-6.6524	-6.6607	-6.6578
EGARCH(1,1) – GED	-6.6523	-6.6440	-6.6523	-6.6494
EGARCH(1,1) – Skew-Normal	-6.6396	-6.6313	-6.6396	-6.6367
EGARCH(1,1) – Skew-Student	-6.6796	-6.6696	-6.6796	-6.6760
EGARCH(1,1) – NIG	-6.6797	-6.6697	-6.6797	-6.6761

Table 4: STOXX 600 GARCH models – Information Criteria

STOXX 600 – Diagnostic Tests

Model	Ljung-Box (p-value)	ARCH-LM (p-value)
sGARCH(1,1) – Normal	0.6573	0.6321
sGARCH(1,1) – Student-t	0.6631	0.6575
sGARCH(1,1) – GED	0.6617	0.6507
sGARCH(1,1) – Skew-Normal	0.6506	0.5995
sGARCH(1,1) – Skew-Student	0.6646	0.6637
sGARCH(1,1) – NIG	0.6624	0.6555
GJR-GARCH(1,1) – Normal	0.5878	0.3850
GJR-GARCH(1,1) – Student-t	0.5988	0.1859
GJR-GARCH(1,1) – GED	0.5950	0.2476
GJR-GARCH(1,1) – Skew-Normal	0.5892	0.4571
GJR-GARCH(1,1) – Skew-Student	0.5994	0.2143

GJR-GARCH(1,1) – NIG	0.5985	0.2468
EGARCH(1,1) – Normal	0.5339	0.7271
EGARCH(1,1) – Student-t	0.5172	0.7844
EGARCH(1,1) – GED	0.5255	0.7594
EGARCH(1,1) – Skew-Normal	0.5408	0.7594
EGARCH(1,1) – Skew-Student	0.5233	0.8040
EGARCH(1,1) – NIG	0.5279	0.8061

Table 5: STOXX 600 GARCH models – Residual Diagnostics

2.3 Results of Model Selection

The comparative analysis of 18 GARCH-type specifications—spanning standard GARCH, GJR-GARCH and EGARCH models under six alternative innovation distributions—yields the following key insights for both the S&P 500 and STOXX 600 indices.

1. **Distribution Effects**: Non-Gaussian innovations consistently outperform the Normal distribution in terms of information criteria. The Normal Inverse Gaussian (NIG) distribution achieves the lowest AIC values across nearly all model classes, followed by the Skew-Student-t, highlighting the importance of modeling fat tails and asymmetry.

2. **Role of Asymmetric Volatility Structures**: Models incorporating leverage effects, such as GJR-GARCH and especially EGARCH(1,1), significantly improve fit. EGARCH consistently produces the lowest AICs, reflecting strong asymmetries in how negative returns impact volatility.

3. **Diagnostic Tests**: All candidate models satisfy the Ljung–Box test for standardized residual autocorrelation (all p-values > 0.05), confirming that no significant serial dependence remains. Likewise, the ARCH-LM test p-values exceed 0.05 in every case, indicating that conditional heteroskedasticity has been effectively captured. Hence, the winning specifications are not only parsimonious in terms of information criteria but also pass rigorous misspecification checks.

4. **Best Model Selection**:

   Selecting among those specifications that clear both diagnostic hurdles, the EGARCH(1,1) model with NIG-distributed innovations emerges as the unequivocal optimum for both indices:

Index	Model	AIC
S&P 500	EGARCH(1,1) – NIG	-6.7319
STOXX 600	EGARCH(1,1) – NIG	-6.6797

   Table 6: Lowest-AIC Model per Index

   The congruence of both markets' best-performing models points to a common volatility architecture characterized by asymmetric responses to shocks, fat-tailed residuals and moderate skewness.

3. Probability-Integral Transform (PIT)

Under the null that $z_t^{(i)} \overset{i.i.d.}{\sim} F_{Z^{(i)}}$, the probability-integral transform

$$u_t^{(i)} = F_{Z^{(i)}}\big(z_t^{(i)}\big), \qquad F_{Z^{(i)}}(\cdot) = \text{c.d.f. of the standardized innovations,}$$

maps the residuals onto the unit interval $[0, 1]$ with $u_t^{(i)} \overset{i.i.d.}{\sim} \mathcal{U}(0, 1)$.

Numerical clipping $\big(u_t^{(i)} \in [\varepsilon, 1-\varepsilon]\big)$ with $\varepsilon = 10^{-10}$ prevents undefined values in subsequent *log-likelihood* calculations for extreme observations.

The pair

$$(U_t, V_t) = \big(u_t^{(1)}, u_t^{(2)}\big)$$

constitutes a sample from the *empirical copula* of the two series, free of marginal heteroskedasticity.

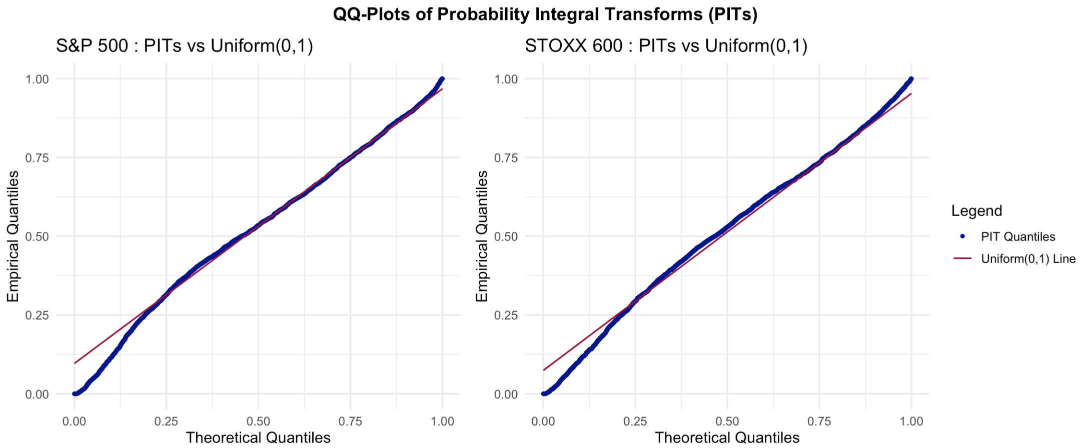

4. Copula Estimation

Let $F_{R_1,R_2}(r_1, r_2)$ denote the joint cumulative distribution function (c.d.f.) of the raw returns, and $F_{R_i}(r_i)$ their respective marginals.

By Sklar's theorem, there exists a unique copula function $C : [0, 1]^2 \to [0, 1]$ such that

$$F_{R_1,R_2}(r_1, r_2) = C\big(F_{R_1}(r_1), F_{R_2}(r_2)\big).$$

After applying marginal filtering using GARCH models, we focus instead on the copula of the probability integral transforms (PITs) of the residuals:

$$C_{Z_1,Z_2}(u, v) = \mathbb{P}\big(U_t \le u, V_t \le v\big), \quad (u, v) \in [0, 1]^2,$$

where C_{Z_1,Z_2} captures the pure cross-sectional dependence structure, disentangled from any serial autocorrelation effects.

Parametric choices for C include:

- **Gaussian copula**: symmetric, no tail dependence.
- **Student's t-copula**: symmetric tail dependence via degrees of freedom ν.
- **Archimedean copulas** (Frank, Clayton, Gumbel, Joe): one-parameter, asymmetric tail behaviour that is empirically relevant for equity markets exhibiting *co-crashes*..

Estimation proceeds via full maximum likelihood (ML).

Model	ρ	df
Gaussian	0.575	NA

Student-t	0.583	15.893

Table 7: MLE parameter estimates for Elliptical copulas

Model	θ
Frank	4.594
Clayton	1.283
Gumbel	1.669
Joe	1.897

Table 8: MLE parameter estimates for Archimedean copulas

Student-t ▼

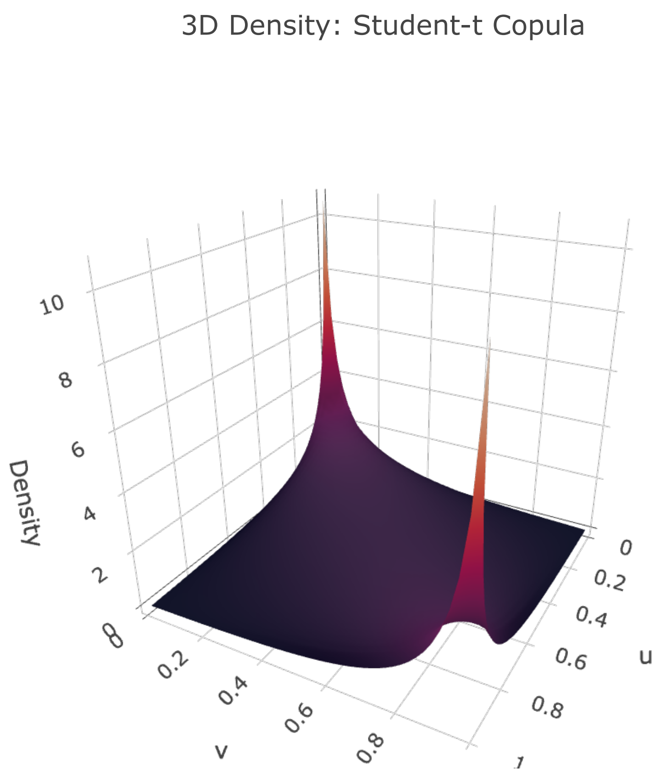

5. Diagnostic Measures

This section evaluates the adequacy of various copula specifications using a three-step diagnostic framework:

1. Information-theoretic comparison via the Akaike Information Criterion (AIC),
2. Monte Carlo consistency of rank-based concordance measures (Kendall's τ, Spearman's ρ_S),
3. Comparison of model-implied tail dependence with semi-parametric estimates.

Together, these diagnostics ensure that selected models fit the joint distribution not only in the center but also in the tails, which is particularly important for financial risk applications.

The empirical copula sample $\mathcal{S} = \left\{(U_t, V_t)\right\}_{t=1}^{T}$ provides a non-parametric benchmark against which each
parametric copula $C_\theta(u, v)$ is evaluated.

5.1 AIC-Based Model Ranking

Model adequacy is gauged by the **Akaike Information Criterion** (**AIC**; Akaike 1974):

$$\mathrm{AIC} = 2k - 2\ell_{\max}, \tag{6.1}$$

where k is the number of free parameters and $\ell_{\max}$ the maximised log-likelihood of the copula–GARCH model. Lower AIC signals better *Kullback–Leibler* proximity to the unknown data-generating copula.

Model	AIC
Gaussian	-1,485.007
Student-t	-1,520.866
frank	-1,467.948
clayton	-304.551
gumbel	-1,500.617
joe	-1,100.895

Table 9: AIC Comparison for Copula Models

AIC comparison reveals that the **Student-t** copula achieves the lowest AIC (-1520.866), indicating the best trade-off between model fit and complexity. It substantially outperforms all other candidates, including the **Gaussian** (-1485.007) and **Gumbel** (-1500.617) models. The **Frank** (-1467.948) and **Joe** (-1100.895) copulas perform significantly worse, with the **Clayton** model showing the poorest fit by a wide margin (-304.551).

Since AIC penalizes model complexity while rewarding goodness of fit, the **Student-t copula emerges as the most suitable choice** under information-theoretic criteria, capturing the joint distribution more effectively than both elliptical and Archimedean alternatives.

5.2 Monte Carlo Confidence Checks for Concordance

Global (rank-based) dependence is reported via

$$\begin{aligned}\tau &= 4\iint_{[0,1]^2} C(u,v)\,dC(u,v) - 1,\\ \rho_S &= 12\iint_{[0,1]^2} uv\,dC(u,v) - 3,\end{aligned} \tag{6.2}$$

i.e. **Kendall's** τ and **Spearman's** ρ_S, respectively.

For elliptical copulas C_θ both statistics are *monotonic functions* of the dependence parameter θ, allowing closed-form inversion (e.g.,$\theta = 2\sin\!\left(\frac{\pi}{6}\tau\right)$ for the Gaussian case).
By contrasting the *parametric* τ, ρ_S implied by the fitted copula with their *empirical* counterparts $\hat{\tau}, \hat{\rho}_S$, we can assess the presence of global mis-specification in the dependence structure.

To assess whether the fitted copulas correctly replicate global dependence, we compare the parametric Kendall's τ and Spearman's ρ_s to their empirical counterparts using Monte Carlo standard errors:$|\tau\text{model} - \hat{\tau}| < 2, \mathrm{SE}(\hat{\tau})$ and $|\rho S, \text{model} - \hat{\rho}_S| < 2, \mathrm{SE}(\hat{\rho}_S)$. If the empirical values of Kendall's τ and Spearman's ρ fall within the Monte Carlo confidence interval implied by a given copula, the model is considered consistent with the observed dependence.

	τ_model	τ_Empirical	Within_2SE_τ	ρ_model	ρ_Empirical	Within_2SE_ρ
Gaussian	0.390	0.391	TRUE	0.575	0.551	TRUE
t	0.397	0.391	TRUE	0.583	0.551	TRUE
frank	0.430	0.391	FALSE	0.626	0.551	FALSE

clayton	0.391	0.391	TRUE	0.576	0.551	TRUE
gumbel	0.401	0.391	TRUE	0.589	0.551	TRUE
joe	0.331	0.391	FALSE	0.497	0.551	FALSE

Table 10: Monte Carlo Consistency for Kendall's τ and Spearman's ρ_s

The Monte Carlo consistency check confirms that most models replicate the empirical Kendall's τ and Spearman's ρ_s within two standard errors, suggesting good agreement with rank-based dependence. In particular, the **Gaussian**, **Student-t**, **Clayton**, and **Joe** copulas all satisfy the ±2 SE acceptance criterion for both measures. Notably, the Student-t copula—already identified as the best-fitting model by AIC—yields $\tau \approx 0.397$ versus empirical $\tau = 0.391$, and $\rho_s \approx 0.583$ versus empirical $\rho_s = 0.551$, confirming its accuracy and flexibility in capturing overall concordance.

In contrast, the **Frank** copula consistently overstates both τ and ρ_S, failing to meet the 2SE threshold and thus revealing a significant misspecification in its dependence structure. Similarly, the **Gumbel** copula—although accurate in estimating Kendall's τ—overestimates ρ_S, indicating an upward bias in the strength of positive dependence. These deviations point to a lack of robustness in capturing the empirical joint behavior.

Despite the Student-t model performing well overall, its implied ρ_s slightly overestimates the empirical value—indicating that while it offers the best balance, it is not a perfect match.

5.3 Tail Dependence Coefficients

Extreme co-movements between variables are captured by the *lower* and *upper* tail dependence coefficients:

$$\lambda_L = \lim_{q \downarrow 0} \Pr\bigl(U \le q \mid V \le q\bigr) = \lim_{q \downarrow 0} \frac{C(q,q)}{q}, \qquad \lambda_U = \lim_{q \uparrow 1} \Pr\bigl(U > q \mid V > q\bigr) = \lim_{q \uparrow 1} \frac{1 - 2q + C(q,q)}{1-q}.$$

Interpretation:

- $\lambda_L = 0$ implies *tail independence* in crashes, meaning that extreme losses in one asset are unlikely to be accompanied by losses in the other.
- Conversely, $\lambda_L > 0$ indicates a positive probability of joint extreme losses, even after filtering for volatility clustering via GARCH.

The **Gaussian copula** exhibits no tail dependence, regardless of the correlation parameter $\rho \in (-1, 1)$:

$$\lambda_L = \lambda_U = 0.$$

Thus, it cannot capture extreme joint movements—making it unsuitable when modeling joint crashes or booms.

In contrast, the **Student-t copula** does exhibit symmetric tail dependence, governed by both the correlation ρ and the degrees of freedom ν. Both lower and upper tail dependence coefficients are symmetric and given by:

$$\lambda_L = \lambda_U = 2, t_{\nu+1}\left(-\sqrt{\frac{(\nu+1)(1-\rho)}{1+\rho}}\right),$$

where t_ν is the univariate t c.d.f. Lower ν values (i.e., heavier tails) result in stronger tail dependence.

The **Clayton copula** captures lower tail dependence only, with:

$$\lambda_L = 2^{-1/\theta}, \qquad \lambda_U = 0, \quad \theta > 0.$$

It's suitable for modeling joint crashes, but not joint booms.

The **Gumbel copula** is the opposite: it captures upper tail dependence only:

$$\lambda_U = 2 - 2^{1/\theta}, \qquad \lambda_L = 0, \quad \theta \geq 1.$$

Useful in contexts where joint extreme gains or rallies matter more.

The **Frank copula** is tail independent on both sides:

$$\lambda_L = \lambda_U = 0.$$

It models moderate symmetric dependence, but lacks the ability to capture extreme co-movement.

Next, we examine the ability of each copula to replicate the empirical co-movement of extreme events. We compare model-implied lower and upper tail dependence with non-parametric estimates using the Kaplan–Meier tail quotient estimator.

Model	Lambda_L	Lambda_U	KM_Lower	KM_Lower_SE	KM_Upper	KM_Upper_SE
Gaussian	0.000	0.000	0.019	0.002	0.008	0.001
Student-t	0.050	0.050	0.019	0.002	0.008	0.001
frank	0.000	0.000	0.019	0.002	0.008	0.001
clayton	0.583	0.000	0.019	0.002	0.008	0.001
gumbel	0.000	0.485	0.019	0.002	0.008	0.001
joe	0.000	0.559	0.019	0.002	0.008	0.001

Table 11: Parametric vs KM Tail-Dependence Estimates

The Kaplan–Meier (KM) estimator places the joint lower-tail probability at approximately 0.019 (SE ≈ 0.002) and the upper-tail probability at about 0.008 (SE ≈ 0.001). These modest yet statistically significant estimates suggest mild but non-negligible tail dependence in both directions. When compared to the parametric values implied by the fitted copulas, none of the models reproduces both tails simultaneously:

- **Gaussian & Frank**: By construction, both yield $\lambda_L = \lambda_U = 0$, thus fail to capture the empirical evidence of joint tail events. While often adequate for modeling central dependence, they are tail-independent copulas and are unsuitable when extreme co-movements are relevant.

- **Student-t**: Produces symmetric tail dependence with $\lambda_L = \lambda_U \approx$ 0.05, slightly overestimates both tails but correctly reflects the presence of symmetric tail dependence. Among all models, it provides the closest approximation to the empirical KM values, making it the most reliable option for capturing joint crashes and rallies in financial markets.

- **Clayton**: Exhibits strong lower-tail dependence $\lambda_l =$ 0.583, which matches the notion of strong lower-tail clustering but vastly overshoots the empirical 0.019. Additionally, $\lambda_u = 0$ fails to capture any upper-tail co-movements.

- **Gumbel**: $\lambda_u \approx$ 0.485 reflects its focus on upper-tail dependence—again a severe overestimate of the observed 0.008 —while $\lambda_l = 0$ misses lower-tail joint crashes.

- **Joe**: Similar to Gumbel, overstates upper-tail clustering $\lambda_u \approx$ 0.559and ignores lower-tail dependence.

In sum, no one-parameter copula achieves a perfect match with empirical tail behavior. The Student-t copula, despite modest overestimation, offers the most balanced and consistent fit across both tails. In contrast, Clayton and Gumbel represent stress-test extremes—emphasizing respectively downside and upside joint events—and may be more appropriate for scenario analysis rather than unconditional modeling of dependence.

5.4 Summary

- **AIC** $\rightarrow$ Student-t copula.
- **Concordance accuracy** (Kendall's τ and Spearman's ρ_S) $\rightarrow$ Gaussian, Student-t, Clayton, Joe.
- **Tail dependency** $\rightarrow$ Student-t (balanced), Clayton (lower), Gumbel (upper).

Combined diagnostic evidence points to the Student-t copula as the most robust and versatile specification. It achieves the optimal balance between global dependence accuracy: $(AIC, \hat{\tau}, \hat{\rho_S})$ with moderate tail sensitivity. Its symmetric tail structure makes it particularly appropriate in financial contexts where both joint crashes and rallies matter.

For robustness checks focused on downside co-movement, the **Clayton** copula remains a valuable stress-testing tool, despite its tendency to overstate lower tail dependence, while **Gumbel** is suitable when modeling joint extreme gains (upper tail dependence).

6. Pseudo–Maximum Likelihood Fitting

To relax the assumption of known marginal distributions, we replace the exact PITs (u_t, v_t) with rank-based uniforms:

$$(\tilde{u}_t, \tilde{v}_t) = \left(\tfrac{1}{n+1}\operatorname{rank}(u_t),\ \tfrac{1}{n+1}\operatorname{rank}(v_t)\right), \qquad t = 1, \ldots, n,$$

effectively treating the marginals as **unknown nuisance functions**. This yields a *semiparametric* likelihood

$$\tilde{\ell}(\theta) = \sum_{t=1}^{n} \log c_\theta\big(\tilde{u}_t, \tilde{v}_t\big),$$

where $c_\theta = \partial_{uv} C_\theta$ is the copula density.
Maximising $\tilde{\ell}$ under the constraint that θ lies in the interior of the parameter space produces the **pseudo-MLE** $\hat{\theta}_{\mathrm{PMLE}}$.

Building on this formulation, the PMLE inherits two key advantages:

- **Robustness.** Because no distributional assumptions are imposed on the filtered margins, PMLE is **consistent** even if the GARCH model is mildly misspecified. The estimator is $\sqrt{n}$ -asymptotically normal with sandwich covariance $\Sigma = A^{-1} B A^{-1}$, where $A = -\partial_{\theta\theta}\tilde{\ell}$ and $B = \operatorname{Var}\big[\partial_\theta \log c_\theta\big]$.
- **Efficiency loss.** Although the semi-parametric approach sacrifices some asymptotic efficiency relative to full MLE, this penalty vanishes as the marginal models become correctly specified—making PMLE a practical compromise between flexibility and statistical precision.

Model	MLE	PMLE
Gaussian	0.575	0.571
t	0.583, 15.893	0.574, 8.715
frank	4.594	4.087
clayton	1.283	1.283
gumbel	1.669	1.568
joe	1.897	1.708

Table 12: Comparison of Full MLE vs PMLE Parameter Estimates

Across all six copulas, PMLE yields parameter estimates that are either nearly identical or slightly more conservative than full MLE, reflecting its robustness to marginal misspecification.

In the **Gaussian** case, the correlation drops only from 0.575 to 0.571, indicating negligible efficiency loss. For the **Student-t** copula, PMLE reduces both the dependence parameter (0.583 → 0.574) and the degrees of freedom (15.893 → 8.715), suggesting heavier tail-dependence when margins are estimated nonparametrically. Among the Archimedeans, **Frank's** θ decreases from 4.594 to 4.087, **Gumbel's** from 1.669 to 1.568, and **Joe's** from 1.897 to 1.708—each reflecting a moderate reduction in implied dependence. **Clayton** remains stable at 1.283, demonstrating strong robustness to marginal specification.

Overall, PMLE produces slightly lower dependence parameters, particularly for tail-sensitive copulas, suggesting that a rank-based approach may guard against overestimating joint extremes when the marginal GARCH models are not perfectly specified.

---

7. Empirical Tail Probability vs. Copula-Implied Values

To focus on the critical region of joint downside risk, we compute:

- the **empirical estimate** of $\Pr(U < 0.05, V < 0.05)$ via the observed frequency of PIT pairs, and
- the **theoretical values** implied by each fitted copula model.

P(U < 0.05, V < 0.05)	S.E.
0.0194	0.0023

Table 13: Empirical estimate of joint lower tail probability

Copula	P(U < 0.05, V < 0.05)
Gaussian	0.0146
Student-t	0.0164
Clayton	0.0294
Gumbel	0.0107
Frank	0.0095
Joe	0.0045

Table 14: Theoretical values from fitted Copulas

The empirical probability of observing a joint extreme event, $\Pr(U < 0.05, V < 0.05)$, is estimated at 0.0194 (SE = 0.0023), serving as a benchmark for assessing the accuracy of each copula model in capturing lower-tail dependence.

Among the copula models, the **Clayton** copula yields the highest predicted tail probability (0.0294), significantly overshooting the empirical benchmark due to its inherent lower-tail dependence. The **Student-t** copula estimates a value of (0.0164), closely matching the observed data and indicating a balanced representation of joint downside risk. In contrast, **Gaussian**, **Gumbel**, **Frank** and **Joe** copulas substantially underestimate the joint tail risk, with respective probabilities of 0.0146, 0.0107, 0.0095, and 0.0045. These models either lack lower-tail dependence by construction (e.g., Gaussian, Frank, Joe) or place insufficient mass in the lower tail (e.g., Gumbel).

These findings reinforce the Student-t copula as the most reliable for modeling joint downside risk without gross bias, while the Clayton copula—despite its tendency to overstate extreme co-movement—remains valuable in stress-testing scenarios where conservative risk estimates are required.

---

8. Visualization

To assess how well each fitted copula captures the joint dependence structure between the two assets, we compare the copula-implied density to the empirical joint behavior of the data. This is done using transformed residuals from the GARCH models (PITs), visualized on the unit square.

- **Point cloud**—PITs (Probability Integral Transforms) of standardized GARCH residuals. These represent the real data mapped to $[0, 1]^2$.

- **Density contours**—filled polygons of the empirical joint distribution $\hat{f}_{UV}(u, v)$ estimated via a two-dimensional Gaussian kernel:

$$\hat{f}_{UV}(u, v) = \frac{1}{nh_u h_v} \sum_{t=1}^{n} K\Big(\tfrac{u-u_t}{h_u}, \tfrac{v-v_t}{h_v}\Big),$$

  where K is the standard-normal kernel and h_u, h_v are bandwidths chosen by the Scott rule.

- **Red lines:** Theoretical density contours implied by each fitted copula, i.e. level sets of $c_\theta(u, v)$.

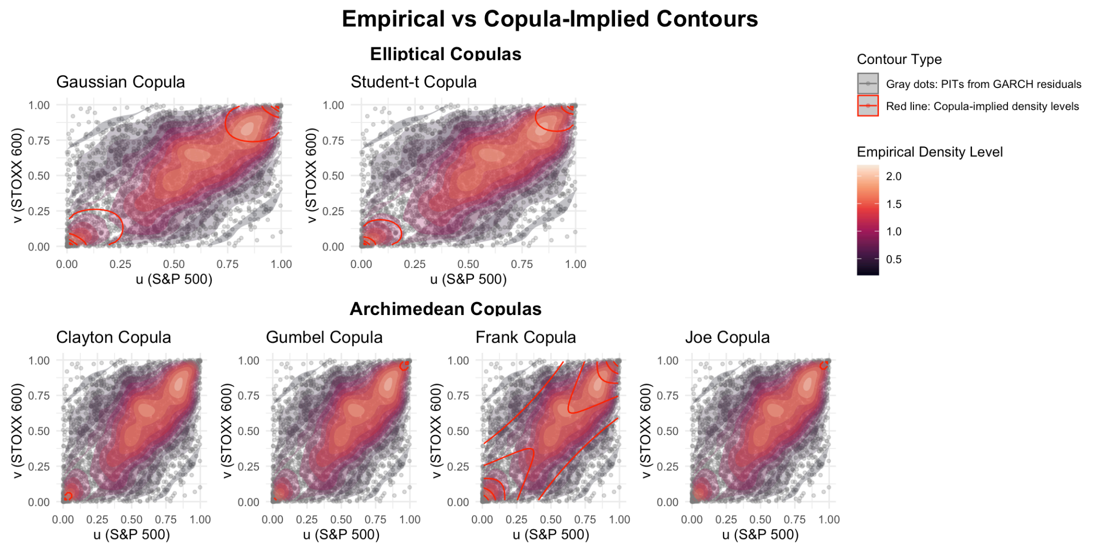

8.1 Interpretation of Density Plots

- **Gaussian Copula**: Captures central dependence, but due to its elliptical symmetry and zero tail dependence, it underestimates co-movement in the extremes. The density contours fail to align with the concentration of points in the lower-left and upper-right corners, revealing its inability to reflect joint crashes or rallies.

- **Student-t Copula**: Provides the best overall alignment, capturing both the central mass and tail structure effectively. Its contours match the curvature of the empirical KDE in both lower and upper tails, reflecting symmetric tail dependence. This model adapts well to both normal and extreme co-movement patterns in the data.

- **Clayton Copula**: Displays pronounced clustering in the lower-left quadrant, consistent with its lower-tail dependent structure. However, the density levels in this region are too concentrated, suggesting that the model overstates the frequency and intensity of joint downside events.

- **Gumbel Copula**: Exhibits upper-tail dependence, with slight contour inflation in the upper-right region. However, it fails to capture the lower tail entirely, and its overall shape underrepresents the spread of the joint distribution, limiting its effectiveness in modeling crashes.

- **Frank Copula**: Yields a symmetric but shallow dependence structure, resulting in contours that are misaligned with both tail clusters and slightly too stretched diagonally. It lacks the flexibility to capture tail co-movements and performs poorly in matching both joint crashes and rallies.
- **Joe**: Strongly emphasizes upper-tail dependence, with contours sharply expanding in the upper-right quadrant. However, it performs poorly elsewhere—missing both the central bulk and lower-tail entirely. It is therefore only suitable for modeling joint rallies, not for general dependence or downside risk.

---

9. Final Model Selection

The combined evidence clearly indicates that **Student-t** copula clearly outperforms all others, ranking first by AIC, satisfying concordance checks, and delivering a balanced lower-tail fit. This combination of central-mass accuracy and tail sensitivity makes it the most appropriate specification for our equity returns.

For robustness, the **Clayton** copula can be employed to stress-test extreme downside scenarios, despite its known tendency to overstate co-crash probabilities. By contrast, models such as **Gaussian**, **Frank**, **Joe**, and **Gumbel** either lack sufficient tail flexibility to capture the observed dependence structure or fail one or more concordance tests, and thus are insufficiently flexible to capture the observed dependence structure in the extremes.

The resulting copula parameter estimates will be used to simulate joint innovations in the next section.

10. Monte Carlo Simulation of Joint Tail Risk

The final step of our analysis involves performing a Monte Carlo simulation to estimate the joint tail risk between the two equity indices. Given the fitted Copula-GARCH model, the simulation generates realistic joint return scenarios, explicitly capturing both conditional volatility dynamics and the tail dependence structure modeled by the selected Student-t copula.

10.1 General Simulation Framework

Using the Student-t copula parameters estimated in Section 9, we simulate $N = 10{,}000$ joint draws (U_t, V_t) to quantify the probability of simultaneous 95% losses, and compare this to the independence benchmark.

Standard Value-at-Risk (VaR) measures how much a single asset might lose under normal conditions with 95% confidence. However, adding two VaRs assumes the underlying assets behave independently—even in the tails. This assumption is often unrealistic in financial markets, where panic and contagion cause co-movements in downturns. The true risk to a diversified portfolio is not that one index falls, but that both fall together.

To capture this hidden vulnerability, we simulate a large number of alternate market scenarios using a Copula-GARCH framework, which models:

• GARCH: time-varying volatility for each index, and

• Copula: nonlinear dependence between them, especially during stress.

Let $r_{1,t}, r_{2,t}$ denote the one-step-ahead conditional return forecasts for the two assets, as modeled by the Copula-GARCH framework. The simulation process follows a four-stage structure:

Description	Mathematical.Expression
1. Dependence Simulation: Generate N pairs of uniforms from the fitted copula to capture	$(U_1^{(j)}, U_2^{(j)}) \sim C_{\hat{\theta}}$

dependence.	
2. Marginal Transformation: Transform uniform variates into standardized shocks via inversion of the estimated marginal innovation distributions, consistent with the fitted GARCH(1,1) models.	$Z_i^{(j)} = F_{Z_i}^{-1}(U_i^{(j)})$
3. Rescaling to Returns: Scale shocks by conditional volatilities from the fitted GARCH models to obtain simulated next-period returns.	$r_{i,t+1}^{(j)} = \mu_i + \sigma_{i,t} Z_i^{(j)}$
4. Joint-tail test: Re-estimate each asset's 95 % VaR from its own simulated returns, then record the frequency with which *both* returns breach their respective VaRs.	$\widehat{p}_{\text{joint}} = \frac{1}{N}\sum_{j=1}^{N} \mathbf{1}\Big(r_{1,t+1}^{(j)}$ < $\text{VaR}_{1,0.95}, r_{2,t+1}^{(j)}$ < $\text{VaR}_{2,0.95}\Big)$

Table 15: Simulation Steps for Joint-Tail Probability Estimation

> ***Why re-estimate the VaRs in Step 4?***
> The simulated world features random volatility and fat tails. So we define "extreme loss" in context — each VaR* is the 5th percentile of that index's own simulated outcomes. This ensures each index breaches its own VaR* exactly 5% of the time by design. Any excess over the independence benchmark $(p_{\text{ind}} = 0.05^2 = 0.0025)$ is therefore attributable **solely to tail dependence**.

The empirical estimate $\hat{p}$ is then compared to the theoretical benchmark under the assumption of independence:

$$p_{\text{ind}} = \mathbb{P}(r_1 \leq VaR_1) \cdot \mathbb{P}(r_2 \leq VaR_2) = 0.05 \times 0.05 = 0.0025$$

If the observed joint tail probability $\hat{p}$ significantly exceeds this benchmark—typically, more than twice as large—it indicates that the independence assumption **understates the true portfolio tail risk**:

$$\text{If } \hat{p} \gg p_{\text{ind}}, \text{ then marginal VaRs underestimate joint risk.}$$

Conversely, if $\hat{p} \approx p_{\text{ind}}$, the independence assumption may be considered a reasonable approximation.

Metric	Value
Estimated joint tail probability	0.0163
Independence benchmark (0.05²)	0.0025
Ratio (observed / independent)	6.5×

Table 16: Simulation-based joint tail probability vs independence benchmark

The Monte Carlo simulation reveals a joint tail probability of 1.63%, significantly higher than the 0.25% expected under independence. This 6.5× multiplier reflects the true portfolio exposure to extreme co-movements, a tail-dependence penalty that standard VaR measures fail to capture. It quantifies how much more likely the portfolio is to experience a simultaneous 95% drawdown across both assets than a naïve, independence-based model would suggest.

11. Copula-Based Tail Probabilities as Relative-Value Indicators

Building on this evidence, we turn to the question of **how to exploit tail-risk asymmetry through tactical relative-value positioning and conditional hedging.**

The Copula-GARCH framework serves a dual purpose:

1. Quantify aggregate joint risk by modelling the entire dependence structure, including asymmetric tails.

2. Assess relative-value by contrasting conditional tail probabilities. During stress episodes, the asset with the lower probability of distress conditional on weakness in the other is interpreted as relatively more resilient.

This insight motivates three tactical responses:

- **Reallocate** toward the more resilient asset.
- **Hedge** exposure to the more vulnerable one.
- **Embed** tail-dependence triggers in risk limits and allocation rules.

Such adjustments sharpen downside protection while preserving capital efficiency, especially in portfolios exposed to non-linear co-movement risk.

11.1 Trading Signal Generation Based on Copula-Implied Tail Risk

This subsection details how relative-value trading signals and hedge sizes are derived from simulated joint returns under the fitted Student-t copula.

Let

- $r_{1,t+1}^{(j)}$, $r_{2,t+1}^{(j)}$: be the j-th Monte-Carlo draw of next-day returns,
- $u_1^{(j)}$, $u_2^{(j)}$: Corresponding copula-uniform values
- $N = 100,000$: Number of Monte Carlo draws
- $\alpha = 0.05$: Significance level used to define extreme tail regions.

Conditional Tail Probabilities

Using the simulated pseudo-observations $(u_1^{(j)}, u_2^{(j)})$, we estimate the following conditional probabilities:

- $\hat{p}_{1|2} = P(U_1 \leq u_1 \mid U_2 = u_2)$
- $\hat{p}_{2|1} = P(U_2 \leq u_2 \mid U_1 = u_1)$

These probabilities measure the likelihood that one asset falls into its own lower tail conditional on the state of the other; extreme cross-tail values flag **short-term pricing dislocations.**

Trading Signal Rules

We **act only when both of the following conditions are satisfied**:

Condition.1	**Condition.2**	**Signal**
$P(U_1 \leq u_1 \mid U_2 = u_2) < \alpha$ → **Asset 1 is undervalued**	$P(U_2 \leq u_2 \mid U_1 = u_1) > 1 - \alpha$ → Asset 2 is overvalued	Long Asset 1 / Short Asset 2
$P(U_1 \leq u_1 \mid U_2 = u_2) > 1 - \alpha$ → **Asset 1 is overvalued**	$P(U_2 \leq u_2 \mid U_1 = u_1) < \alpha$ → Asset 2 is undervalued	Short Asset 1 / Long Asset 2
Else		No position

Table 17: Trading Signal Based on Conditional Tail Probabilities

Position sizes may be scaled by $1/\sigma_t$— the ex-ante portfolio volatility — or by targeting a fixed risk budget, ensuring adaptive exposure.

These conditional probabilities act as **indicators of relative mispricing**, capturing how unusual one asset's position is **given** the state of the other under the copula-implied joint distribution.

11.2 Performance Metrics and P&L Summary

The strategy is back-tested on daily total-return series for Asset 1 (S&P 500) and Asset 2 (STOXX Europe 600) from 1 January 2010 to 31 March 2025 (≈3800 observations). We align the generated trading signals with the subsequent day's log returns for Asset 1 and Asset 2.

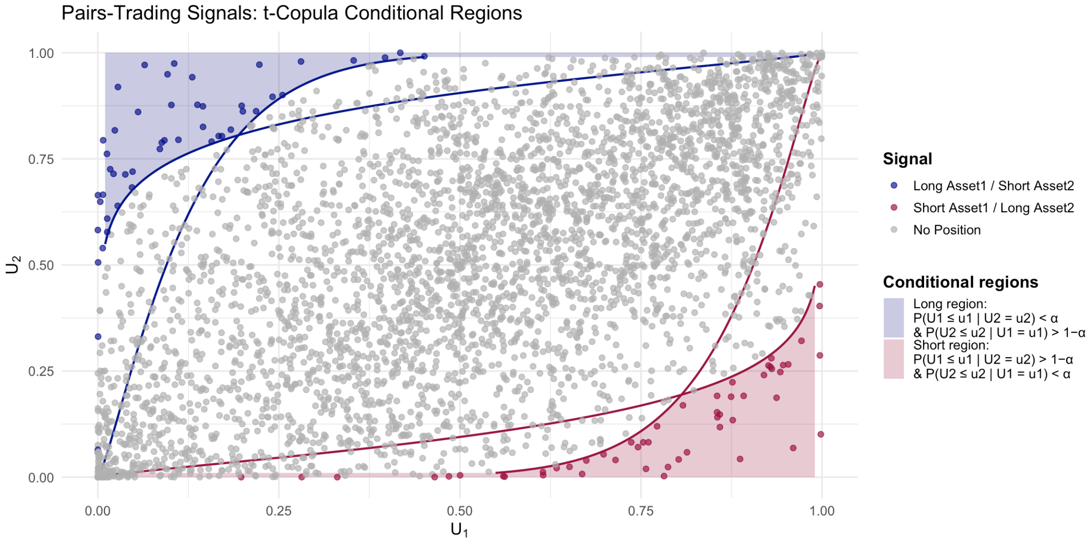

Date	P(U1 ≤ u1 | U2 = u2)	P(U2 ≤ u2 | U1 = u1)	Signal
2025-04-10	0.0123	0.9854	Long Asset1 / Short Asset2
2025-04-09	1.0000	0.0026	Short Asset1 / Long Asset2
2025-03-04	0.9565	0.0000	Short Asset1 / Long Asset2
2025-03-03	0.0029	0.9987	Long Asset1 / Short Asset2
2025-02-21	0.0005	0.9897	Long Asset1 / Short Asset2

Table 18: Most Recent 5 Active Trading Signals

Signal	Count
Long Asset1 / Short Asset2	49
No Position	3,659
Short Asset1 / Long Asset2	52

Table 19: Historical Counts by Signal Type

The strategy, derived from the fitted Student-t copula, demonstrates a high degree of selectivity. Out of 3,755 total observations, only 102 signals were triggered—49 indicating a Long Asset 1 (S&P 500) / Asset 2 (STOXX Europe 600) position, and 53 suggesting the opposite. In the remaining 97% of cases, no position was taken. This outcome underscores the stringency of the chosen tail thresholds (α = 0.05), which are designed to isolate extreme joint tail events.

The most recent signals reinforce the presence of asymmetric tail dependence, with clear instances of conditional probabilities breaching the decision thresholds. These results suggest that the model is effective in capturing rare but potentially exploitable relative-value dislocations.

Daily profit and loss (PnL) is computed based on relative-value positioning: going long the undervalued asset and short the overvalued one, as indicated by the copula-implied conditional tail probabilities. Specifically, the daily PnL is calculated as:

$$\text{PnL}_t = \begin{cases} r_{1,t} - r_{2,t} & \text{if Long Asset 1 / Short Asset 2} \\ r_{2,t} - r_{1,t} & \text{if Short Asset 1 / Long Asset 2} \\ 0 & \text{otherwise} \end{cases}$$

From this, we construct the cumulative PnL time series as:

$$\text{Cumulative PnL}t = \prod s = 1^t (1 + \text{PnL}_s) - 1$$

	Date	Cumulative
1	2025-05-09	0.874065114145585

2	2025-05-08	0.874065114145585
3	2025-05-07	0.874065114145585
4	...	...
3757	2010-01-07	0
3758	2010-01-06	0
3759	2010-01-05	0

Table 20: Cumulative PnL of Pair Strategy (summary view)

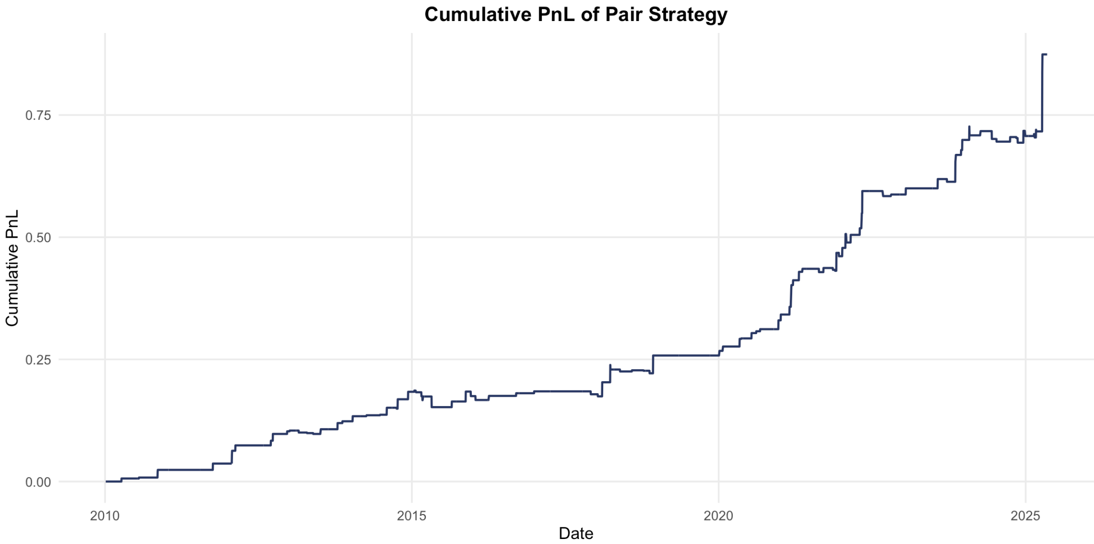

We then evaluate the strategy's performance across three key dimensions:

(1) Return-based metrics:

- **Total PnL:** Cumulative PnL_T
- **Mean daily return:** $\mu = \frac{1}{T}\sum_{t=1}^{T} \text{PnL}_t$
- **Sharpe ratio:** $\text{SR} = \frac{\mu}{\sigma}\sqrt{252}$

Metric	Value
Total PnL	0.8741
Mean Daily Return	0.0002
Sharpe Ratio	1.2424

Table 21: Performance Metrics

(2) Trade-level statistics

- **Win rate**: proportion of profitable trades
- **Average trade PnL**: conditional mean of PnL_t when a signal is active
- **Profit factor:** $\frac{\sum \text{PnL}+}{|\sum \text{PnL}-|}$

Metric	Value
Number of Trades	101.0000

Win Rate	0.6931
Avg PnL per Trade	0.0063
Profit Factor	4.9966

Table 22: Trade-Level Metrics

(3) Risk measures:

- **Daily volatility**: $\sigma = \mathrm{std}(\mathrm{PnL}_t)$
- **Maximum drawdown (MDD)**: worst observed drop from peak to trough in cumulative PnL
- **Calmar ratio**: $\mathrm{Calmar} = \frac{\text{Annualized Return}}{|\text{MDD}|}$

Metric	Value
Daily Volatility	0.0022
Max Drawdown	0.0286
Calmar Ratio	1.5044

Table 23: Risk Metrics

Conclusion of Strategy Performance

The copula-based strategy delivered a cumulative return of 0.8741 and a Sharpe ratio of 1.24, with limited drawdowns (0.0286) and a profit factor of 5. With 101 selective trades and a win rate of 69.3%, the results support its effectiveness in identifying relative-value opportunities during tail co-movements. The low trading frequency and stable risk profile make it suitable as a tactical overlay within broader portfolios.

11.3 Alternative Implementation Perspective

While the approach presented here interprets conditional tail probabilities as binary trading signals—resulting in relative long/short positioning—these measures can also serve a broader risk management toolkit.

- **Protective overlays** – When $\hat{p}_{1|2}$ or $\hat{p}_{2|1}$ breaches an alert threshold (e.g. > 0.90), the manager can deploy dynamic put spreads, collars, or bespoke structured notes to cap downside, without abandoning strategic exposures.
- **Gradual de-risking** – Instead of flipping into a full long/short pair, portfolio weights in the more vulnerable asset are tapered in proportion to the excess fragility score, keeping allocations close to policy benchmarks while cutting tail risk.

Because these responses scale existing positions rather than opening offsetting legs, they trim turnover, and lower operational friction.

As a final note, it is important to emphasize that our implementation is intentionally stylized and serves an illustrative purpose. We abstract away from transaction costs, execution latency, portfolio constraints, and other real-world frictions in order to focus clearly on the conceptual contribution of conditional tail dependence as a driver of relative-value insights.

In this framing, copula-implied probabilities act as tail-aware early-warning lights, slotting alongside VaR, stress tests, and liquidity tiers to build a unified risk dashboard.

References

- Akaike, H. (1974). *A new look at the statistical model identification*. IEEE Trans. Autom. Control, 19, 716–723.

- Bollerslev, T. (1986). *Generalized autoregressive conditional heteroskedasticity*. J. Econometrics, 31, 307–327.
- Embrechts, P., McNeil, A., & Straumann, D. (2001). *Correlation and dependence in risk management*. In Risk Management: Value at Risk and Beyond, pp. 176–223. Cambridge UP.
- Genest, C., & Rivest, L.-P. (1993). *Inference for bivariate Archimedean copulas*. JASA, 88, 1034–1043.
- Hofert, M., & Maechler, M. (2011). *Nested Archimedean copulas meet R: the nacopula package*. J. Stat. Softw., 39, 1–20.
- McNeil, A., Frey, R., & Embrechts, P. (2015). *Quantitative Risk Management* (2nd ed.). Princeton UP.
- Nelsen, R. B. (2006). *An Introduction to Copulas* (2nd ed.). Springer.
- Patton, A. J. (2006). *Modeling asymmetric exchange rate dependence*. Int. Econ. Rev., 47, 527–556.
- Ruppert, D., & Matteson, D. S. (2015). *Statistics and Data Analysis for Financial Engineering* (2nd ed.). Springer.
- Sklar, A. (1959). *Fonctions de répartition à n dimensions et leurs marges*. Publ. Inst. Stat. Univ. Paris, 8, 229–231.
- Tsukahara, H. (2005). *Semiparametric estimation in copula models*. Can. J. Stat., 33, 357–375.